Atmos. Chem. Phys. Discuss., https://doi.org/10.5194/acp-2018-1254
Manuscript under review for journal Atmos. Chem. Phys.
Discussion started: 11 December 2018

Atmospheric Chemistry and Physics Discussions

Regional New Particle Formation as Modulators of Cloud Condensation Nuclei and Cloud Droplet Number in the Eastern Mediterranean

Panayiotis Kalkavouras[1,2], Aikaterini Bougiatioti[1,2], Nikos Kalivitis[1], Maria Tombrou[3], Athanasios Nenes[2,4,5], and Nikolaos Mihalopoulos[1,2]

[1]Env. Chemical Processes Lab., Dept. of Chemistry, Univ. of Crete, Heraklion, 71003, Greece
[2]Institute of Environmental Research & Sustainable Development, National Observatory of Athens, Palea Penteli,15236, Greece
[3]Department of Physics, Univ. of Athens, Athens, 15784, Greece
[4]Laboratory of Atmospheric Processes and their Impacts, Schools of Architecture, Civil & Environmental Engineering, École Polytechnique Fédérale de Lausanne, 1015, Lausanne, Switzerland
[5]Institute for Chemical Engineering Science, Foundation for Research and Technology Hellas, Patras, 26504, Greece

Correspondence to: athanasios.nenes@epfl.ch; abougiat@noa.gr

Abstract

A significant fraction of atmospheric particles that serve as cloud condensation nuclei (CCN), and furthermore as cloud droplets are thought to originate from the condensational growth of new particles formed from the gas phase. Here, particle number size distributions (<850 nm), aerosol chemical composition and meteorological parameters were studied during 7 years of continuous measurements (June 2008 to May 2015) at a remote background site of the eastern Mediterranean. 162 NPF episodes were recorded and analyzed to assess the impact of NPF on CCN and cloud droplet number concentration (CDNC) formation. A new metric is introduced to quantitatively determine the initiation and duration of the influence of NPF on the CCN spectrum. Annually, NPF days were found to increase CCN concentrations between 40 and 50% in the 0.2-1.0% supersaturation range. CCN perturbations from NPF are found to occur in the afternoon, relatively later in the winter and autumn than in the summer. Introducing the observed aerosol size distributions together with chemical composition into an established cloud droplet parameterization showed that the supersaturations that develop however are much lower (below 0.1%) for typical boundary layer dynamics (width of the vertical velocity distribution ~ 0.3 m s^{-1}) and NPF is found to enhance CDNC by 7 to 12.5%. This considerable contrast between CCN and CDNC response is in part from the different supersaturation levels considered, but also because supersaturation drops from increasing CCN because of water vapor competition effects. The low cloud supersaturation further delays the appearance of NPF impacts on CDNC to clouds formed in the late evening and nighttime – which carries important implications for the extend and types of indirect effects induced by NPF events. An analysis based on CCN concentrations using prescribed supersaturation can provide much different, and

Atmos. Chem. Phys. Discuss., https://doi.org/10.5194/acp-2018-1254
Manuscript under review for journal Atmos. Chem. Phys.
Discussion started: 11 December 2018

even misleading, conclusions and should be avoided. The proposed approach here offers a simple, yet highly effective way for a more realistic impact assessment of NPF events on cloud formation.

1. Introduction

Cloud condensation nuclei (CCN) and cloud droplet formation constitutes the direct microphysical link between aerosols and clouds. Quantifying how changes in aerosols affect global clouds, precipitation and climate is limited by the large number of processes and scales that need to be captured in models (Stevens and Feingold, 2009; Pöschl et al., 2010; Seinfeld et al., 2016; Cecchini et al., 2017). New particle formation (NPF), the process during which new particles are formed directly from the gas-phase, is thought to significantly shape the distribution of CCN throughout the atmosphere (Pierce and Adams 2007; Westervelt et al., 2013; Gordon et al., 2017). Although initially too small (1–2 nm; Kerminen et al., 2012) to act as CCN, particles from NPF can grow to sufficient size and hygroscopicity over a period of few hours to days and eventually act as efficient CCN.

Field studies have demonstrated substantial local enhancement in CCN number from NPF. For example, Wiedensohler et al. (2009) observed that the CCN size distribution was dominated by the growing nucleation mode (above 80%) in a highly polluted region around Beijing. Sihto et al. (2011) found in Hyytiälä that NPF increase the CCN concentrations in the evening of a NPF day by 70-110% depending on the supersaturation level, while Rose et al. (2017) observed that CCN concentrations were increased by 168 to 996% at Chacaltaya during NPF events. Additionally, model investigations suggest atmospheric NPF to be an important contributor to CCN, and thereby to aerosol-cloud-climate interactions. Spracklen et al. (2008) have shown that boundary layer (BL) particle formation can cause an increase in global BL CCN concentrations at 0.2% supersaturation by 3-20%, and by 5-50% at 1.0% supersaturation, respectively. Merikanto et al. (2009) found that 45% of global low-level cloud CCN at 0.2 % supersaturation originates from nucleation. Moreover, Westervelt et al. (2014) estimated an average global increase in the boundary-layer CCN number concentration at 0.2% supersaturation due to nucleation ranging between 49 and 78%.

NPF events followed by growth to CCN-sized particles are observed to take place frequently and over relatively large spatial scales in continental boundary layers, including forested areas at mid and high latitudes, other remote continental regions, urban areas and even highly-polluted environments (e.g. Kulmala and Kerminen, 2008). NPF events are long known to occur in marine environments from rapid dimethylsulphide (DMS) oxidation above clouds (Bates et al., 1987; Kreidenweis et al., 1991; Katoshevski et al., 1999), oxidation of biogenic alkyl-halides and VOC in near-coastal areas (e.g., O'Dowd et al., 2002; Vaattovaara et al., 2006) and

Atmos. Chem. Phys. Discuss., https://doi.org/10.5194/acp-2018-1254
Manuscript under review for journal Atmos. Chem. Phys.
Discussion started: 11 December 2018

cloud outflow regions associated with convection (e.g. Hermann et al., 2003). NPF within marine boundary layers can strongly affect CCN concentrations at all cloud-relevant supersaturations (Kalivitis et al., 2015; Kalkavouras et al., 2017). When these small particles however are mixed within the boundary layer, they may subsequently grow to CCN-relevant sizes, or even act as CCN in strongly convective clouds (Fan et al., 2013; Wang et al., 2016).

A thorough assessment of NPF impacts on CCN levels requires knowledge of all events and subsequent microphysical processing that occurred throughout the path of an air-mass. Observationally, this is almost impossible to carry out; one can therefore only quantify the CCN concentration perturbation, or enhancement, above "background" levels that existed prior to an NPF event (Peng et al., 2014; Wu et al., 2015; Ma et al., 2016). Although conceptually straightforward, studies differ in the approach used to define the initiation of an NPF event (e.g., a strong enhancement in total particle number, the shape of the size distribution), the pre-event CCN concentration (e.g., a 30-minute or 1 hour-average CCN concentration before the initiation time) and also the metric used to quantify the CCN enhancement from an NPF event (e.g., peak enhancement, a time-averaged enhancement, and the size defining the lower limit of CCN activation). Furthermore, observational studies quantify CCN enhancements from measurements of aerosol number size distribution; the link to CCN concentrations is done by using a prescribed (or calculated) "critical diameter" above which all particles act as CCN in clouds. Studies widely vary in the approach used to determine d_c, so additional considerations are required between assessments. Theoretically, d_c depends on the level of supersaturation that develops in clouds and the chemical composition of the particles (Seinfeld and Pandis, 2006). Often, d_c is prescribed between 50 and 150 nm, corresponding roughly to clouds with maximum saturation levels between 1.0%, and 0.1%, respectively (Kerminen et al. 2012). However, clouds are not characterized by a constant supersaturation, rather exhibit variable levels that instantaneously adjust to the intensity of cloud updrafts and the CCN spectra (Nenes and Seinfeld, 2003; Hudson et al., 2014). It is clear that all the above conventions need careful consideration, as they can affect the magnitude and duration of CCN enhancement for each event.

Asmi et al. (2011) at the Pallas GAW station in northern Finland estimated the contribution of NPF to CCN concentration. The method adopted was to subtract the concentration of particles larger than 80 nm diameter (N_{80}) at the end of the NPF, from the average N_{80} before the NPF influence (defined from the time where the NPF started up to where the nucleation mode particles reach 80 nm diameter). A similar approach was used to quantify the enhancement from NPF to particles larger than 50, and 100 nm (N_{50}, N_{100}, respectively). The relative enhancement of N_{50}, N_{80}, and N_{100} from NPF was 160±270%, 210±110%, and 50±130%, respectively. Kerminen et al. (2012) calculated the CCN concentrations using the particle number size

Atmos. Chem. Phys. Discuss., https://doi.org/10.5194/acp-2018-1254
Manuscript under review for journal Atmos. Chem. Phys.
Discussion started: 11 December 2018

distributions, for diameters above 50, 80, 100 and 150 nm. The contribution of any NPF event was determined from the ratio of the maximum particle number concentration (N_{max}) that develops during an event over the particle number concentration (N_{prior}) prior to the event and the maximum particle number concentration (N_{max}) that develops. N_{prior} is a one-hour average concentration prior to the appearance of the freshly formed nucleation mode particles, while N_{max} is a maximum one-hour average concentration during an event. In Hyytiälä, $N_{50(max)}$ / $N_{50(prior)}$ and $N_{100(max)}$ / $N_{100(prior)}$ presented an increase of 317% and 202%, respectively, in CCN concentration. The approach of Kerminen et al. (2012) has been used in China (Peng et al., 2014), where the contribution of NPF events to CCN at 0.2% supersaturation was 6% on regional sites, while Wu et al. (2015) using 2-h averaging in Melpitz, Germany found that NPF enhance CCN number concentration 63, 66, and 69% for 0.1, 0.4, and 0.6% supersaturation, respectively.

Apart from impacting solely on CCN concentrations, NPF events can also impact on direct aerosol-cloud interactions and climate-relevant properties. According to Sullivan et al. (2018) regional NPF can lead to cloud dimming, and thus, regional warming, at least during periods with high NPF frequency over the comparatively polluted area of Midwestern U.S.A. Furthermore, it is clear that the timing of the initiation of the NPF event and the subsequent growth of particles to CCN and eventually droplets is of utmost importance, as the time delay between the different processes actually limits the time during which the albedo of clouds is affected by NPF. In reality, the total contribution of nucleation process (including indirect effects) to a present-day net short-wave radiation in the atmosphere, depends on the rate in which the emissions of gas-phase compounds responsible for nucleation and subsequent growth, as well as of primary particles acting as a sink for nucleated particles, throughout an NPF day.

Although most prior observation studies linked NPF to CCN number enhancement, very few of them actually link NPF to the process of cloud droplet formation and cloud droplet number. The latter distinction is important, given that droplet number in clouds exhibit a sub-linear response to aerosol increases, owing to the elevated competition for water vapor and reduction in cloud supersaturation. The understanding of NPF impacts on CCN levels may therefore provide a biased view on its potential impact on droplet number (N_d) and the aerosol indirect effect. Using cloud droplet parameterizations to interpret observed aerosol size distribution data, however, may allow one to address this issue. Kalkavouras et al. (2017) illustrated this issue by using a "conventional" approach to quantify CCN enhancement (with a critical diameter at which all particles act as CCN depended on observed composition and a prescribed supersaturation) and reporting much higher CCN number enhancements (~87%) for two sites in the eastern Mediterranean (Santorini and Finokalia) than in cloud droplet number, N_d,

Atmos. Chem. Phys. Discuss., https://doi.org/10.5194/acp-2018-1254
Manuscript under review for journal Atmos. Chem. Phys.
Discussion started: 11 December 2018

(~12%) during two consecutive NPF episodes. The reason for this 8-fold discrepancy is in the drastically different supersaturation used to quantify CCN enhancement (0.2, 0.4, 0.6, and 0.8%) than what was computed for cloud droplet number (0.10 and 0.13% for updraft velocities of 0.3 m s^{-1} and of 0.6 m s^{-1}, respectively).

This study follows up on the initial work of Kalkavouras et al. (2017) and quantifies the impact of NPF on CCN levels and cloud droplet number in the Eastern Mediterranean atmosphere over 7 years of continuous measurements (June 2008 to May 2015) of aerosol number size distributions and chemical composition. From this data, we aim to (*i*) quantify the seasonality and contribution of atmospheric NPF to the production of newly CCN in the eastern Mediterranean marine atmosphere, (*ii*) characterize the differences between nucleated particles and their relative contribution to the CCN budget, and, (*iii*) investigate the NPF impacts on cloud droplet number concentration (N_d) and on maximum supersaturation (s_{max}) formed in clouds in the vicinity of Finokalia. In the process of addressing these goals, we consider all the issues regarding the calculation of cloud supersaturation and event characteristics that affect the NPF impact calculations.

2. Methodology

2.1 Experimental site

From June 2008 to May 2015, measurements were performed at the atmospheric observation station of the University of Crete at Finokalia, Crete, Greece (35° 20′N, 25° 40′E; 50 m from the shore and 250 m above sea level (a.s.l.)). The monitoring station of Finokalia (http://finokalia.chemistry.uoc.gr/), is located at the top of a hill over the coastline, in the northeast part of the island of Crete, facing the Aegean Sea in the wide north sector. Since the site was established in 1993, Finokalia experiences two characteristic periods during the year; the dry period from April to September, and the wet one from October to April. The dry period is dominated by strong winds of N/NW direction (up to 90%, originating from Central and Eastern Europe and Balkans) of speed exceeding 10 m s^{-1}. The wet period is characterized by limited prevalence of the N/NW sector, and significant transport from Sahara (S/SW winds; occurrence up to 20%). An extensive description of the site and prevailing meteorology can be found in Mihalopoulos et al., 1997.

2.2 Aerosol composition and size distribution

Number size distribution of particles having mobility diameters from 9 to 848 nm (scanned range) were measured with a 5 min time resolution, using a custom-built scanning mobility particle sizer (SMPS; TROPOS-Type, Wiedensohler et al., 2012). The system is a closed-loop, with a 5:1 ratio between the aerosol and sheath flow, and it comprises a Kr-85 aerosol neutralizer (TSI 3077), a Hauke medium differential mobility analyzer (DMA), and a TSI-3772

Atmos. Chem. Phys. Discuss., https://doi.org/10.5194/acp-2018-1254
Manuscript under review for journal Atmos. Chem. Phys.
Discussion started: 11 December 2018

condensation particle counter (CPC). The sampling was made through a PM_{10} sampling head and the sample humidity was regulated to a relative humidity below 40% using Nafion® dryers in both the aerosol and sheath flow, and thereafter charged via Kr-85 neutralizer, and introduced into the DMA. By setting different voltages in the DMA, particles of different electrical mobility are selected and their particle number concentration can be measured. The fluctuation of voltage yields an electrical particle mobility distribution, which can be inverted into a particle number size distribution. The recorded number size distributions were corrected for particle losses by diffusion on the various parts of the SMPS following the recommendations by Wiedensohler et al. (2012). Three different types of calibration were performed for the SMPS, namely DMA voltage supply calibration, aerosol and sheath flows calibrations and size calibrations.

The complete dataset of particle size distributions was checked for the presence of NPF events, identified by a sudden of nucleation-mode particles (i.e. those with diameters below 25 nm), that lead to a continuous increase in larger particle concentrations over a short period of time (usually less than 4h). The NPF event progression is characterized by the relative changes of the three particle modes, "nucleation" (diameter less than 25 nm), "Aitken" (diameter between 25 and 100 nm), and "accumulation" (diameter larger than 100 nm). The concentration of particles in each mode is obtained from each SMPS size distribution using an algorithm to parameterize each particle's mode with a multi log-normal distribution function (Hussein et al., 2005), as follows:

$$N_{nucleation}=\int_0^{25} n(d_p)\mathrm{d}d_p \approx \sum_{i_9}^{i_{25}} \Delta N_i \quad (1)$$

$$N_{Aitken} = \int_{25}^{100} n(d_p)\mathrm{d}d_p \approx \sum_{i_{25}}^{i_{100}} \Delta N_i \quad (2)$$

$$N_{Accumulation} = \int_{100}^{\infty} n(d_p)\mathrm{d}d_p \approx \sum_{i_{100}}^{i_{848}} \Delta N_i \quad (3)$$

where $n(d_p)$ is the aerosol number size distribution, ΔN_i is its binned approximation from the SMPS data and i_9, i_{100}, i_{848} are the SMPS size bins that correspond to particles of 9, 100 and 848 nm, respectively. The upper and lower sizes are limits of size detection for the particular SMPS.

From the period between June 2008 and December 2011, the bulk aerosol chemical composition of PM_{10} was measured in parallel with the size distributions using daily 24-h quartz fiber filters (PALL Tissuquartz, 2500 QAT 47 mm). Samples were analyzed for water-soluble ions after extraction with nanopure water. The solutions acquired were first filtered using syringe filters (PALL IC Acrodisc® (PES), 0.45 µm, 13 mm) to remove any non-soluble species and subsequently analyzed using ion chromatography (IC) for anions (Cl^-, Br^-, NO_3^-, SO_4^{2-}) and cations (K^+, Na^-, NH_4^+, Mg^{2+}, Ca^{2+}), using the procedure of Bardouki et al. (2003).

Atmos. Chem. Phys. Discuss., https://doi.org/10.5194/acp-2018-1254
Manuscript under review for journal Atmos. Chem. Phys.
Discussion started: 11 December 2018

Furthermore, the PM_{10} quartz filters were analyzed for organic and elemental carbon (Carbon Aerosol Analysis Lab Instrument, SUNSET Laboratory Inc.) using the EUSAAR 2 protocol of analysis (Cavalli et al., 2010). For the estimation of the fine particulate matter fraction (PM_1) chemical composition, the respective concentrations of sulfates, organics, and ammonium from the bulk PM_{10} are considered using the approach presented in Bougiatioti et al. (2009). From May 2012 to May 2015, the mass and chemical composition of non-refractory submicron aerosol particles (SO_4^{2-}, NO_3^-, NH_4^+,Cl^-, and organics) was provided by an Aerodyne Research Inc. Aerosol Chemical Speciation Monitor (ACSM; Ng et al., 2011), with a 30 min time resolution. Throughout the measurement period, ambient air was drawn into the ACSM through a PM_1 Sharp Cut Cyclone (BGI Inc.) at 3.5 l min^{-1}.

2.3 Cloud Condensation Nuclei (CCN)

Measurements of cloud condensation nuclei (CCN) concentration (cm^{-3}) between 0.2 and 1.0% supersaturation, were conducted using a Droplet Measurement Technologies (DMT) constant flow streamwise thermal-gradient CCN counter (CFSTGC; Roberts and Nenes, 2005), from November 2014 to May 2015. The CFSTGC is composed of a cylindrical diffusion chamber in which supersaturation is generated and controlled by the air flow rate, pressure, and a streamwise temperature gradient maintained by a heater and a set of thermoelectric coolers (Roberts and Nenes, 2005; Lance et al., 2006). The air flow rate used was 0.5 L min^{-1} with a sheath-to-aerosol flow ratio of 10:1, and a top-bottom column difference, ΔT, between 4 and 15 K. Concentrations were measured at each supersaturation (0.2, 0.38, 0.52, 0.66, and 0.73%) for 15 min, yielding a CCN spectrum consisting of 5 different supersaturations approximately every hour. Calibration of the instrument supersaturation was performed by determining the minimum diameter of classified ammonium sulfate aerosol that activates at given chamber flow rate, ΔT and chamber pressure, following the procedure of Bougiatioti et al. (2009). The CCN instrument was calibrated numerous times throughout the campaign. For the lower supersaturation, the relative variability between calibrations did not exceed 1%, whereas for the highest supersaturation the variability was under 4%. As CCN concentrations during the measurement period rarely exceeded 5,000 cm^{-3}, no correction for water vapor depletion inside the CFTGC chamber was deemed necessary (Lathem and Nenes, 2011).

2.4 Calculation of CCN concentrations from size distribution data

As in numerous prior studies, CCN concentrations can be calculated from the observed number size distributions by integrating the SMPS data from a characteristic diameter d_c to the largest size particles measured:

$$\mathrm{CCN}\ (d_c) = \int_{d_c}^{\infty} n(d_p)\mathrm{d}d_p \approx \sum_{i_{dc}}^{i_{848}} \Delta N_i \qquad (4)$$

Atmos. Chem. Phys. Discuss., https://doi.org/10.5194/acp-2018-1254
Manuscript under review for journal Atmos. Chem. Phys.
Discussion started: 11 December 2018

where i_{dc} is the SMPS size bin that contains d_c and i_{848} is the bin with the largest particles measured by the SMPS. Instead of prescribing d_c (as done in other studies), we link it to a desired supersaturation level, s_c, using κ-Köhler theory:

$$d_c = \left(\frac{4A^3}{27\kappa s_c^2}\right)^{1/3}, \quad A = \frac{4M_w\sigma_w}{RT\rho_w},$$

where M_w is the molar mass of water, σ_w is the surface tension of water, R is the universal gas constant, T is the temperature, and ρ_w is the density of water. CCN concentrations are then taken as being equal to the concentration of particles with diameter above d_c (Kalkavouras et al., 2017). The aerosol hygroscopicity parameter, κ, is calculated assuming that it is a mixture of an organic and inorganic component with volume fraction ε_{org}, ε_{inorg} and characteristic hygroscopicity κ_{org}, κ_{inorg} respectively. Past studies at Finokalia have suggested that assuming κ_{org}=0.16 and κ_{inorg}=0.6 reproduce CCN to within 2% on average, but exhibit some size dependence (Bougiatioti et al., 2009; 2011). For 4 NPF days during August and September 2012, the combined processing of the concurrent CCN and ACSM data during NPF events provides the size-resolved κ (Fig. S1), which can be used to assess the validity of using a common κ for all sizes (supersaturations). For supersaturations below 0.2%, the size-resolved κ from the CCN data is higher by 23% compared to the bulk κ from the ACSM data, while for supersaturations between 0.2 and 0.4%, CCN-derived values agree quite well with bulk chemical composition data (slope 0.94), but with considerable scatter. For supersaturations above 0.4% κ derived from the chemical composition data exhibits on average an overestimation bias of 38.5%. Altogether, the κ trends suggest that the composition of particles tends to increasingly deviate (or vary) from the bulk as they get smaller (i.e., with higher supersaturation) – indication of enrichment by organics, often observed for NPF-derived particles (e.g., Cerully et al., 2011). The large scatter at around 0.4% supersaturation can be attributed to chemical composition fluctuations, given that concentrations are affected by both the fresh organic-rich and aged sulfate-rich modes, more at least than found in the higher or lower supersaturation CCN. Overall however, this level of hygroscopicity error, is not expected to induce substantial errors in CCN concentration predictions, as demonstrated in the closure study below; a size-dependent consideration of hygroscopicity is therefore deemed unnecessary.

We subsequently test the aforementioned approach for calculating CCN from chemical composition and size-distribution measurements (Eq. 4) against direct CCN measurements (Section 2.3) collected from September 2014 to March 2015. The degree of "CCN closure" is assessed with 5 minute-averaged data at 0.38, 0.52, 0.66, and 0.73% supersaturation (Fig.S2). The measured values of CCN at each supersaturation correlate strongly with the predicted values, when considering all the available data. With increasing supersaturation, *s*, the value of

Atmos. Chem. Phys. Discuss., https://doi.org/10.5194/acp-2018-1254
Manuscript under review for journal Atmos. Chem. Phys.
Discussion started: 11 December 2018

R^2 increased and the scattering of data decreased (Table S1). For the lowest supersaturations (0.38 and 0.52%), there is an overestimation (22%) of predicted CCN concentrations – consistent with the fact that using bulk κ, which is higher than the "real" size-dependent κ, would lead to slight overestimations in CCN. Interestingly enough, although these κ biases increase with decreasing size, the overestimation and scatter in CCN is decreased, for the higher supersaturations (0.66 and 0.73% - estimated and measured values agree within 10%) because an increasingly larger fraction of the aerosol activates so the error in absolute CCN number is diminished. Regardless of supersaturation, CCN prediction errors and scatter do not seem to exceed 40%; these are considered minor, especially within the context of droplet number calculations – because the former exhibit a strongly sub-linear response to CCN changes in the eastern Mediterranean (e.g., Kalkavouras et al., 2017; Bougiatioti et al., 2016) which means that CCN errors translate to much smaller errors in CDNC.

2.5 Cloud droplet formation calculations

From knowledge of the aerosol hygroscopicity, size distribution and cloud vertical velocity, we can determine the droplet number (N_d) and maximum supersaturation for clouds forming in the vicinity of Finokalia, during all NPF events. Such calculations are useful to directly link aerosol with cloud droplet number in NPF-influenced clouds, and, determine the "cloud-relevant" supersaturations for which CCN perturbation calculations are relevant. For such calculations we use the droplet parameterization based on the "population splitting concept" of Nenes and Seinfeld (2003), later improved by Fountoukis and Nenes (2005), Barahona et al. (2010), and Morales and Nenes (2014). These formulations provide a rapid and accurate calculation of droplet number that forms in cloud updrafts, and largely captures the droplet numbers that form in ambient clouds (e.g., Ghan et al., 2011; Morales-Betancourt et al., 2011). When calculating N_d, the size distribution is described using a sectional representation (Nenes and Seinfeld, 2003) derived directly from the SMPS distribution data, similar to what was done in Kalkavouras et al. (2017). Observations of updraft velocity are not available at Finokalia for the time period examined, but published measurements and model simulations suggest that the distribution of vertical velocities in cloudy boundary layers in the region show a dispersion of σ_w = 0.2-0.3 m s^{-1} during the period of northerly (Etesian) winds (Tombrou et al., 2015; Dandou et al., 2017), consistent with the dynamics observed in cloud-capped marine boundary layers (e.g. Meskhidze et al., 2005; Ghan et al., 2011). Thus, we can use the characteristic updraft velocity approach of Morales and Nenes (2010) when applying the droplet parameterization to obtain velocity PDF-averaged values of cloud droplet number concentration (CDNC) and s_{max}. Moreover, a sensitivity test also considers a more vigorous boundary layer (σ_w = 0.6 m s^{-1}), following Kalkavouras et al. (2017).

Atmos. Chem. Phys. Discuss., https://doi.org/10.5194/acp-2018-1254
Manuscript under review for journal Atmos. Chem. Phys.
Discussion started: 11 December 2018

Furthermore, we determine the relative contribution of aerosol chemical composition, $\varepsilon\kappa$, and aerosol number concentration, εN_{total}, to variations in droplet number using a propagation of variance (Sullivan et al., 2016; Bougiatioti et al., 2016; 2017),

$$\varepsilon N_{total} = \frac{\left(\overline{\frac{\partial N_d}{\partial N_{total}}}\sigma N_{total}\right)^2}{\sigma^2 N_d} \quad (5) \quad \text{and} \quad \varepsilon\kappa = \frac{\left(\overline{\frac{\partial N_d}{\partial \kappa}}\sigma\kappa\right)^2}{\sigma^2 N_d} \quad (6)$$

where $\sigma^2 N_d = (\overline{\frac{\partial N_d}{\partial N_{total}}}\sigma N_{total})^2 + (\overline{\frac{\partial N_d}{\partial \kappa}}\sigma\kappa)^2$ is the variance of the droplet number, σN_{total} is the standard deviation of the total aerosol number, $\sigma\kappa$ is the standard deviation of the hygroscopicity parameter, and $\overline{\frac{\partial N_d}{\partial N_{total}}}, \overline{\frac{\partial N_d}{\partial \kappa}}$ represent the average sensitivity of N_d to aerosol number and hygroscopicity, respectively throughout a NPF episode, as calculated by the droplet parameterization (Bougiatioti et al., 2016; 2017). The relative contribution of κ, and N_{total} to the N_d droplet number variation is estimated only during periods with high temporal resolution in chemical composition in order to capture the diurnal variability of κ (ACSM measurements, June 2012 to May 2015).

2.6 Back-trajectories and meteorological data

For the entire dataset, three-dimensional back-trajectories have been calculated to determine the origin and trajectories of air-masses arriving at Finokalia. The HYSPLIT4 model (Hybrid Single-Particle Lagrangian Integrated Trajectory; http://ready.arl.noaa.gov/HYSPLIT.php) were used for the analysis (Stein et al., 2015), initialized with meteorological conditions from GDAS (0.5° resolution), were calculated at several heights (100, 500, and 1000 m above ground level (a.g.l.)), with a duration of 48 hours. The back-trajectories are important for understanding the provenance of the different air masses and how they related to the occurrence and evolution of NPF events. Meteorological parameters, as wind speed and direction, temperature, relative humidity, and solar radiation were also continuously monitored during the study period, by the automatic weather station installed at Finokalia at 2 m a.g.l., and the time resolution for all of the measurements was 5 minutes (http://finokalia.chemistry.uoc.gr/).

3. Results and discussion

3.1 Aerosol chemical composition and hygroscopicity during NPF events

162 NPF episodes were recognized (Kalivitis et al., 2018) and the chemical composition of submicron particulate matter during these episodes was primarily composed of sulfate, contributing on average by 39±8% to the total estimated PM_1 mass as derived from the respective bulk PM_{10} 24-h quartz fiber filters, and by 51±12% as derived from the ACSM high-resolution measurements, respectively. Moreover, regarding the organic material the contribution was found to be in the order of 38±10% and 44±12%, respectively indicating that

Atmos. Chem. Phys. Discuss., https://doi.org/10.5194/acp-2018-1254
Manuscript under review for journal Atmos. Chem. Phys.
Discussion started: 11 December 2018

the relative abundance of sulfate, and organics dictate to a high extent the hygroscopic and cloud-activating properties of submicron particles over Finokalia. Sulfate contributed to a greater fraction of the aerosol during autumn (average contribution 43±7%), and to a lesser extent in springtime (35±9%), whilst organic material contributed more during winter (44±14%) and in autumn (32±8%), respectively.

Following Section 2.4, κ, was calculated using the chemical composition data. The predicted κ derived from the estimated PM_1 varied from 0.34 to 0.57, with a mean value of 0.48±0.04, while when the ACSM data were considered, κ varied from 0.20 to 0.45, with a mean value of 0.36±0.06. This difference regarding the κ is due to the lower concentrations of organics and sulfate from ACSM data. Mean κ values were estimated to be somehow lower in winter and higher during autumn, while in spring and summer the average aerosol hygroscopicity exhibited generally similar values. Indicatively, the diurnal variability of the κ derived from the chemical composition analysis and from the CCN data for supersaturations below 0.2, and for supersaturations ranging from 0.2 to 0.4, 0.4 to 0.5, and 0.6 to 0.7% on 29 August 2012 is presented in Figure S3. It can be seen that κ tended to decrease throughout the early morning hours (6:00 to 9:00 LT) for each critical supersaturation probably owing to the downward transport of secondary organic aerosol (SOA) during the boundary layer mixing, whilst at some point after noon, κ begun to augment probably linked to the formation of particulate sulfate during this period. As expected, lower supersaturation levels are associated with higher κ values, indicating that smaller particles were much less hygroscopic than larger ones, with the difference being of 0.2 κ units between the lower (under 0.2%) and the maximum supersaturation (0.6-0.7%). This feature has been attributed to the enrichment of organic material in sub-100 nm particles (Kalivitis et al., 2015). The chemically-derived κ from the ACSM measurements generally does not present any remarkable fluctuation, and it seems to converge with the CCN-derived κ values of lower supersaturations. This constant character of the chemically-derived κ, may be an evidence that using prescribed levels of supersaturation or critical diameters to calculate CCN concentrations can provide a biased influence of NPF events on CCN, since there is a clear dependence between the chemical composition and the size of a particle.

3.2 Characteristics and interpretation of the Finokalia NPF events

In all studies to date (summarized in the introduction), NPF impacts on CCN concentrations is based on analysis of the evolution of the aerosol size distribution over time, to quantify *i*) how long it takes before freshly-formed particles in a given air-mass reach CCN-relevant sizes, and, *ii*) the degree to which CCN concentrations are augmented from the NPF. Here we present in detail the corresponding methodology used to interpret the NPF data from Finokalia, by applying to a "representative" type-I NPF event (according to the Dal Maso et al., 2005

classification) observed at Finokalia on 29 August 2012 (Fig. 1). Regarding the intensity, it was a strong episode, since according to Zhang et al. (2004) N_{total} (where N_{total} is the number of particles larger than 9 nm) exceeds 10,000 cm^{-3} for at least 1h (in Fig. 3, N_{total} exhibits values exceeding 10,000 cm^{-3} between 10:00 to 15:30 LT). Subsequent growth of the aerosol generates a characteristic "banana shape" in the time-series of diurnal particle number concentration (Fig. 1a). The episode was characterized by a burst in particle number concentration in the 9 to 25 nm diameter range (nucleation mode), and enables a robust determination of the starting time (t_{start}) of the NPF event. Following Leino et al. (2016), we calculated half-hour median concentrations of the nucleation mode particles from the measurement data, since the half-hour median concentration was deemed sufficient to determine the t_{start}. When plotting the time series of the intermediate nucleation mode particles, the NPF is distinctly visible as the particle concentrations rapidly increase from 3,850 to just over 17,000 cm^{-3} over a 2.5 h period starting at 8:30 LT (Fig 1b). The nucleation mode particles peak at 11:00 LT (see Fig. 1c), without any visible change in Aitken-mode concentrations until after 11:30 LT. This increase, in conjunction with the decrease of the nucleation mode particles in number, strongly suggests the transfer of nucleation-mode to Aitken-mode particles from condensation and coagulation. The NPF event is said to terminate when the nucleation mode particles start to decrease. The appearance and formation of the nucleation mode particles are linked to the onset of solar radiation (Fig. 2). Afterwards, particles continued to grow in size for several hours, exceeding 100nm in diameter at 21:30 LT. Following the methodology of the mode-fitting (Hussein et al., 2004; Kulmala et al., 2012) the nucleation mode particles exhibited a growth rate of 3.7 nm h^{-1}, while the formation rate value of particles in the nucleation mode was 2.0 cm^{-3} s^{-1} (Kulmala et al., 2012), which are well in the range of the representative values reported by Kalivitis et al. (2018) at Finokalia site.

To quantify the impact of NPF on CCN concentrations, the following approach is used. From the time-series of the aerosol size distribution and chemical composition that spans each NPF event, the time-series of CCN concentration for a number of supersaturations *s*, CCN_s, is calculated following Section 2.4. We then determine the starting time, t_{start}, and its corresponding CCN concentration, $CCN_{s,}\ t_{start}$. The enhancement of CCN from the NPF at supersaturations, R_s, is then calculated by normalizing the CCN time series with $CCN_{s,}\ t_{start}$ for each NPF event, $R_s = \frac{CCN_s}{CCN_{s,t_{start}}}$. By definition, R_s is equal to unity at t_{start} and theoretically should remain so until the "wave" of new particles (from the new particles) reaches a large enough size to influence CCN_s.

Figure 3a, presents the evolution of the R_s for each supersaturation against aerosol number concentrations, before, during and after the event. Prior to 8:30 LT (t_{start}) and 5 hours later (13:30 LT), R_s displays a similar pattern for all supersaturations, with values ranging from 0.46

Atmos. Chem. Phys. Discuss., https://doi.org/10.5194/acp-2018-1254
Manuscript under review for journal Atmos. Chem. Phys.
Discussion started: 11 December 2018

to 1.30 (average 0.83±0.17) according to the conceptual model. This pattern reveals that during the morning hours and until 13:30 LT, the estimated CCN concentrations exhibit almost equal values for each supersaturation, since the denominator is constantly the same. At 13:30 LT, R_s acquires different values in a given supersaturation as depicted in Figure 3a. This time is crucial in order to estimate the initiation of the influence on the potential CCN due to NPF, and is termed the "decoupling time", t_{dec}. We determine t_{dec}, and therefore the period (i.e. start and end) of intense NPF impact on CCN spectrum, based on the temporal evolution of the relative dispersion (RD) of the R_s for all supersaturations (Fig. 3b). RD was calculated by diving the standard deviation of the instantaneous values of R_s (at 0.38, 0.52, 0.66, 0.73, and 1.00% supersaturation) with their average value. RD is useful, at it is highly sensitive to the introduction and evolution of particles from NPF as they transit the distribution over the resolved supersaturation range. It is said that NPF influences the CCN as long as the RD exceeds the envelope of (low) values seen during the initial stages of the NPF event. Indeed, from 08:30 to 13:30 LT, the RD is low (less than 0.1), and rapidly increases at 13:30 LT and on – indicative of the large spread in R_s from the influence of NPF on the larger supersaturations; therefore 13:30 LT corresponds to the t_{dec}. The impact of NPF on the CCN spectrum is terminated when the RD drops to values seen prior to t_{dec} (21:30 LT, see Fig. 3b), presumably when the NPF has evenly affects CCN concentrations at all *s* levels. The elevated RD seen after 23:00 LT may be a result of residual NPF particles mixing in the airmasses sampled at Finokalia, or a result of other small-scale variations (from local sources) in the CCN spectrum.

Subsequently, we calculate the evolution of R_s before and after t_{dec} for each supersaturation on 29 August 2012 (Fig. 3a). Specifically, "before" is the time period between t_{start} and t_{dec}, whereas "after" is the period from the t_{dec} until the end of CCN production (21:30 LT). This variation of the R_s can be equivalent to the percentage contribution of CCN owing to NPF. The R_s was estimated to be 0.94±0.08, 1.02±0.09, 1.04±0.09, 1.03±0.09, and 0.99±0.08 prior to the starting of the CCN production (i.e. between 8:30 and 13:30 LT), and 1.09±0.60, 1.21±0.52, 1.25±0.43, 1.26±0.40, and 1.39±0.32 for 0.38, 0.52, 0.66, 0.73, and 1.0% supersaturation, respectively after 13:30 LT until the end of the production. The time intervals and t_{dec} are driven by the processes that affect the aerosol number distributions (i.e. coagulation and condensation), and hence affect the CCN population. Assuming a constant growth rate (3.7 nm h^{-1}) for particles with diameter smaller than 100 nm, we approach the time which the new particles after the t_{start} are able to grow to the respective d_c (35 to 67 nm for *s* 1.0 to 0.38%) and act as CCN. This time fluctuates from 2.7 to 10.5 h in the 1.0-0.38% supersaturation range, showing that larger particles (67 nm) start to "feel" the influence from NPF late in the afternoon (19:00 LT). t_{dec} is later for supersaturations below 0.7%, and this difference may occur due to the change of the growth

Atmos. Chem. Phys. Discuss., https://doi.org/10.5194/acp-2018-1254
Manuscript under review for journal Atmos. Chem. Phys.
Discussion started: 11 December 2018

rate, which has been reported to increase with an increasing particle diameter (Paasonen et al., 2018). The R_s exhibits almost similar mean values after the t_{dec} until 21:30 LT, for 0.38, 0.52, 0.66, and 0.73% supersaturation. Thus, the number of the newly-formed particles which reach the CCN-size (d_c varying from 43 to 67 nm) is independent from *s*, indicating that the newly-formed particles in this size range may exhibit similar chemical composition (internal mixture), or could be merely that particle number in the size range between 43-67 nm particles increased more or less to the same extent, after the t_{dec}. The subsequent percentage contribution of NPF into CCN population at the same time period was calculated to be 16, 19, 20, 22, and 40% for the above-mentioned supersaturations, respectively. The first four contributions are similar, since the d_c spans from 67 nm for 0.38% to 43 nm for 0.73%, respectively. Regarding the *s* of 1.0%, the aerosol sizes are even smaller (~35 nm), and the contribution of NPF on CCN increases considerably. These contributions are suggestive of the convolution of NPF with condensational growth of both fresh and preexisting ("background") particles to produce CCN size range particles, introducing a bias which can reach up to 50% regarding the exact activation of particles solely originating from the NPF. The amount of the "background" particles, which take place into the processes of activation from newly-formed particles to CCN, was calculated by subtracting the mean value of the concentration of particles in the nucleation mode from t_{start} until 11:30 LT (the formation of nucleation mode particles ceased - Fig. 1a) and the respective mean value2 hours prior to the t_{start}.

The procedure outline in section 3.2 is repeated for the all the 161 remaining NPF episodes to determine the relative contribution of the NPF episodes to the R_s and subsequently to the CCN budget. The comprehensive results are presented in Table S2, and an extensive seasonal analysis in the Supplementary Material 3.3 (SM 3.3). Altogether, when considering all 162 NPF episodes we found that, the average contribution of NPF to the CCN budget over eastern Mediterranean varied from 39 to 69% in the 0.38-1.0% supersaturation range, and displayed a seasonal variation (Fig. 4). In winter, t_{start} was observed during daytime (median 11:00 LT), followed by t_{dec} 2.5 hours later. The contribution on CCN production due to atmospheric NPF and growth was estimated to be 47, 47, 48, 50, and 54% for 0.38, 0.52, 0.66, 0.73 and 1.0% supersaturation (Fig. 4), respectively. For spring and summer, t_{start} exhibited a median value at 10:00 LT, and 9:00 LT, respectively, whilst the t_{dec} was on average 2.5 hours after the t_{start}. The CCN production for associated with the nuclei growth to larger sizes increase by almost 40% for both seasons (Fig. 4), and for the aforementioned supersaturations. Finally, throughout autumn, t_{start} was detected in the morning (median 9:30 LT), followed by t_{dec} on average 3.5 hours after the t_{start}, whereas the NPF episodes elevated the CCN numbers by 46, 47, 52, 55, and 69% (Fig. 4) for each supersaturation, respectively. Hence, according to the above conceptual model, NPF taking place in the eastern Mediterranean may considerably influence

Atmos. Chem. Phys. Discuss., https://doi.org/10.5194/acp-2018-1254
Manuscript under review for journal Atmos. Chem. Phys.
Discussion started: 11 December 2018

CCN numbers (compared to levels prior to t_{dec}), at cloud supersaturations encountered in this environment.

3.4 Impact of NPF on droplet number and cloud formation

Following the proposed methodology (Section 2.5), we estimated the number of droplets (N_d) and the maximum supersaturation (s_{max}) that would form in a cloud, based on the aerosol number size distribution (N_{total}), chemical composition (κ), and updraft velocity (σ_w) throughout each NPF event. Results of N_d are shown in Figure 5 for updraft velocities of 0.3 m s^{-1} (bottom) and of 0.6 m s^{-1} (top), whereas Figure 6 depicts the corresponding s_{max} during the "representative" NPF event recorded at Finokalia on 29 August 2012. As expected, the higher updraft velocity generates larger values of both s_{max}, and N_d. On the time period between 8:30-17:25 LT, which includes the formation and growth hours of the episode (8:30-11:00 LT), as well as the starting of the CCN influence due to NPF (13:30 LT), the arrival of the air mass is followed by a depression in N_d (relative mean decrease 7.9±2.9% for σ_w=0.3 m s^{-1} and 13.5±3.9% for σ_w= 0.6 m s^{-1}). Concurrently, there is a slight increase in the maximum supersaturation (relative mean increases4.7±2.1% for σ_w=0.3 m s^{-1} and 6.9±2.3% for σ_w= 0.6 m s^{-1}). Both trends are related to decreases in accumulation mode aerosol number, related to processes other than NPF (growth of the boundary layer, and dry deposition) – as the latter has not had the chance to influence particles that act as CCN in clouds. N_d exhibits the minimum value at 17:25 LT (Fig. 5) and corresponds to when droplet formation begins to "feel" the particles generated from NPF. Hereafter, this time will be expressed as t_{Nd} (Fig. 5). There is a time lag between t_{dec} and t_{Nd}, since particles formed in an NPF event need sufficient time to grow into CCN-relevant sizes, and subsequently into a cloud droplet. After t_{Nd}, s_{max} is negatively correlated with N_d for both updraft velocities, owing to the increasing competition for water vapor from the growing number of CCN. For both updraft velocities, the increase of N_d until the sunset (around 21:30 LT) was similar and on the order of 21.9±6.5%, leading to a simultaneous decrease of s_{max} by 11.8±2.7%. Water vapor competition effects can be assessed by comparing N_d at sunset with the CCN for s_{max} at t_{Nd} (where competition effects from the NPF-generated particles are vanishingly small). Using this approach, we find that competition effects suppress N_d by 20% for σ_w=0.3 m s^{-1} and 12.3% for σ_w=0.3 m s^{-1}. It is worth noting that, if s_{max} did not vary over the period of N_d influence, the increase of N_d from the t_{Nd} until 21:30 LT was similar for both σ_w and merely of 5.5±2.5%, since the competition for water vapor is restricted considerably. This clearly shows that the prescription of a constant supersaturation in the CCN analysis may lead to biased results regarding the impact of NPF on regional clouds. Since N_d does not increase significantly until midnight, it is clear that most of the impact of the NPF is on nocturnal clouds, which carries important implications for the formation of drizzle and structure of the boundary layer in the following day.

Atmos. Chem. Phys. Discuss., https://doi.org/10.5194/acp-2018-1254
Manuscript under review for journal Atmos. Chem. Phys.
Discussion started: 11 December 2018

The degree to which N_{total} and κ variations influences N_d variability can be expressed by calculating the relative contribution of the total aerosol number, and the hygroscopicity to the droplet number using the equations (4), (5), and (6) in section 2.5. The results are displayed in Table S4. We find that N_d varies from t_{Nd} to midnight by 30 cm^{-3} for σ_w equal to 0.3 m s^{-1}, and 35 cm^{-3} for σ_w equal to 0.6 m s^{-1}. 68% of this variance can be attributed to aerosol number and the remaining 32% to changes the chemical composition. The above procedure, when carried out for the 161 remaining NPF episodes, provides consistently similar results (Results depicted in Table S3) for both updraft velocities examined. A detailed summary of the analysis by episode and season is presented in the Supplementary Material 3.4 (SM 3.4).

4. Summary and Conclusions

The aerosol particle number size distributions along with chemical composition and meteorological parameters were studied at a remote background site in the Eastern Mediterranean over a 7-year period in order to quantify how regional new particle formation (NPF) events modulate the concentration of aerosol, cloud condensation nuclei (CCN), droplet number and maximum supersaturation developed in clouds of the region.

Overall, 162 NPF episodes were recorded with the majority occurring during spring and summer (32 and 30.8%, respectively), few during winter (14.8%) and the rest (22.4%) during autumn. The timing and duration of NPF influences on the CCN spectrum and cloud droplet number were accurately determined using a set of new statistical metrics derived from the observational data. Wintertime NPF events were found to start around 11:00 LT and begin affecting the CCN spectrum 3 hours into the event, while in springtime were initiated one hour earlier and increased CCN concentrations 2.5 hours into the event. During summer, recorded NPF events started the earliest (9:30 LT) and the impact on CCN concentrations occurred roughly 2 h after, while in autumn NPF episodes occurred between 9:30 and 10:00 LT, but with the largest delays in observing CCN impacts - 3h 30 min after the start of the event. Overall, when accounting for all NPF episodes, we found that the average increase on CCN levels (0.38-1.0% supersaturation) from NPF over eastern Mediterranean ranged from 37 to 69%.

When the observed size distributions and chemical composition are used in conjunction with a cloud droplet parameterization, the impact of NPF on N_d differs considerably from the CCN-based analysis. Regardless of season, we find that the maximum supersaturation developed in typical boundary layer clouds (updraft velocities of the order of 0.3 m s^{-1}) vary between 0.07% and 0.12%, giving cloud droplet number increases of 7% to 13%. This 4 to 10-fold decrease in N_d sensitivity to NPF (compared to what is deduced from the CCN analysis) is primary from the actual cloud supersaturation being much lower than the prescribed levels in the CCN analysis. N_d sensitivity to NPF however is further reduced during the evolution of NPF events

565 owing to their increased competition for water vapor when forming cloud droplets (the droplet response can be suppressed by almost 1/5 compared to assuming constant supersaturation throughout the NPF). The lowest impact on N_d is observed during summer, as this season exhibits the highest aerosol concentrations prior to NPF events - that either act as CCN or grow to become so during an event. Pre-existing particles have been estimated to contribute up to 570 50% of the activated CCN during summer, denoting the importance of background conditions. A striking consequence of the low cloud supersaturations is that NPF impacts on N_d are observed much later in the event, typically in the late afternoon (after 16:00 LT), and that N_d is relatively insensitive to increases in CCN during the course of an event owing to the competition effects for water vapor. Thus, the impacts of NPF events on eastern Mediterranean 575 clouds occur during the late evening and nighttime. Although such N_d enhancements may limit the short-term impact of NPF on shortwave cloud forcing – it may reduce cloud drizzle and promote stabilization of the marine boundary layer with potentially important implications for the overall boundary layer structure (e.g., Rosenfeld et al., 2006) in days following NPF events.

Perhaps one of the most important findings of this study is the importance of constraining the 580 levels of supersaturation that are generated in ambient clouds, and the diurnal characteristics of the influence during NPF events. Choosing prescribed levels of supersaturation or diameters to define CCN concentrations can provide substantially biased or incomplete insights on the influence of NPF events on regional clouds, the hydrological cycle and climate. The approach presented here offers a simple and highly effective paradigm for quantifying the potential 585 impacts of NPF events on clouds, with tools available to interested researchers upon request.

Author contributions

AK, NK and NM contributed measurements. AN and AB conceived the study and developed the analysis tools, AN, AB, PK and NM carried out the analysis and wrote the paper. All authors commented on the manuscript.

590 **Acknowledgments**

This research is co-financed by Greece and the European Union (European Social Fund- ESF) through the Operational Programme «Human Resources Development, Education and Lifelong Learning» in the context of the project “Reinforcement of Postdoctoral Researchers” (MIS-5001552), implemented by the State Scholarships Foundation (IKY). This study also received 595 financial support from the PANhellenic infrastructure for Atmospheric Composition and climatE change” (MIS 5021516) which is implemented under the Action “Reinforcement of the Research and Innovation Infrastructure”, funded by the Operational Programme

"Competitiveness, Entrepreneurship and Innovation" (NSRF 2014-2020) and co-financed by Greece and the European Union (European Regional Development Fund). We also acknowledge project PyroTRACH (ERC-2016-COG) funded from H2020-EU.1.1. - Excellent Science - European Research Council (ERC), project ID 726165

References

Asmi, E., Kivekäs, N., Kerminen, V.-M., Komppula, M., Hyvärinen, A.-P., Hatakka, J., Viisanen, Y., and Lihavainen, H.: Secondary new particle formation in Northern Finland Pallas site between the years 2000 and 2010, Atmos. Chem.Phys., 11, 12959–12972, doi:10.5194/acp-11-12959-2011.

Barahona, D., West, R. E. L., Stier, P., Romakkaniemi, S., Kokkola, H., and Nenes, A.: Comprehensively accounting for the effect of giant CCN in cloud activation parameterizations, Atmos. Chem. Phys., 10, 2467–2473, doi:10.5194/acp-10-2467-2010, 2010.

Bardouki, H., Liakakou, H, Economou, C., Sciare, J., Smolík, J., Ždímal, V., Eleftheriadis, K, Lazaridis, M., Dyef, C., and Mihalopoulos, N.: Chemical composition of size-resolved atmospheric aerosols in the eastern Mediterranean during summer and winter, Vol. 37, Issue 2, Pages 195-208, doi:10.1016/S1352-2310(02)00859-2, 2003.

Bates, T. S., Charlson, R. J., and Gammon, R. H.: Evidence for the climatic role of marine biogenic sulphur, Nature 329, 319-321,doi:10.1038/329319a0, 1987.

Bougiatioti, A., Fountoukis, C., Kalivitis, N., Pandis, S. N., Nenes,A., and Mihalopoulos, N.: Cloud condensation nuclei measurements in the marine boundary layer of the Eastern Mediterranean: CCN closure and droplet growth kinetics, Atmos. Chem.Phys., 9, 7053–7066, doi:10.5194/acp-9-7053-2009, 2009.

Bougiatioti, A., Nenes, A., Fountoukis, C., Kalivitis, N., Pandis, S. N., and Mihalopoulos, N.: Size-resolved CCN distributionsand activation kinetics of aged continental and marine aerosol,Atmos. Chem. Phys., 11, 8791–8808, doi:10.5194/acp-11-8791-2011, 2011.

Bougiatioti, A., Zarmpas, P., Koulouri, E., Antoniou, M., Theodosi, C., Kouvarakis, G., Saarikoski, S., Mäkelä, T., Hillamo, R., and Mihalopoulos, N.: Organic, elemental and water-soluble organiccarbon in size segregated aerosols, in the marine boundary layerof the Eastern Mediterranean, Atmos. Environ., 64, 251–262,2013.

Bougiatioti, A., Bezantakos, S., Stavroulas, I., Kalivitis, N., Kokkalis, P., Biskos, G., Mihalopoulos, N., Papayannis, A., and Nenes, A.: Biomass-burning impact on CCN number, hygroscopicity and cloud formation during summertime in the eastern Mediterranean, Atmos. Chem. Phys.,16,7389-7409, doi:10.5194/acp-16-7389-2016, 2016.

Bougiatioti, A., Argyrouli, A., Solomos, S., Vratolis, S., Eleftheriadis, K., Papayannis, A., and Nenes, A.: CCN activity, variability and influence on droplet formation during the HygrA-Cd campaign in Athens, Atmosphere 2017, 8(6), 108, doi.org/10.3390/atmos8060108.

Cavalli, F., Viana, M., Yttri, K. E., Genberg, J., and Putaud, J.-P.: Toward a standardised thermal-optical protocol for measuring atmospheric organic and elemental carbon: the EUSAAR protocol, Atmos. Meas. Tech., 3, 79-89, doi:10.5194/amt-3-79-2010, 2010.

Cecchini, M. A., Machado, L. A. T., Andreae, M. O., Martin, S. T., Albrecht, R. I., Artaxo, P., Barbosa, H. M. J., Borrmann, S., Fütterer, D., Jurkat, T., Mahnke, C., Minikin, A., Molleker, S., Pöhlker, M. L., Pösch, U., Rosenfeld, D., Voigt, C., Weinzierl, B., and Wendisch, M.: Sensitivities of Amazonian clouds to aerosols and updraft speed, Atmos. Chem. Phys., 17, 10037-10050, doi:10.5194/acp-17-10037-2017, 2017.

Cerully, K. M., Raatikainen, T., Lance, S., Tkacik, D., Tiitta, P., Petäjä, T., Ehn, M., Kulmala, M., Worsnop, D. R., Laaksonen, A., Smith, J. N., and Nenes, A.: Aerosol hygroscopicity and CCN activation kinetics in a boreal forest environment during the 2007 EUCAARI campaign, Atmos. Chem. Phys., 11, 12369-12386, doi:10.5194/acp-11-12369-2011, 2011.

Dal Maso, M., Kulmala, M., Riipinen, I., Wagner, R., Hussein, T., Aalto, P. P., and Lehtinen, K.E. J.: Formation and growth of fresh atmospheric aerosols: eight years of aerosol size distribution data from SMEAR II, Hyytiälä, Finland, Boreal Environ. Res., 10, 323–336, 2005.

Fan, J., Leung, R., Rosenfeld, D., Chen, Q., Li, Z., Zhang, J., and Yan, H.: Microphysical effects determine macrophysical response for aerosol impacts on deep convective clouds, PNAS, 110 (48) E4581-E4590; doi:10.1073/pnas.1316830110, 2013.

Fountoukis, C., and Nenes, A.: Continued development of a cloud droplet formation parameterization for global climate models, J.Geophys. Res., Vol. 110, D11212, doi:10.1029/2004JD005591, 2005.

Gerasopoulos, E., Kouvarakis, G., Vrekoussis, M., Kanakidou, M., and Mihalopoulos, N.: Ozone variability in the marineboundary layer of the eastern Mediterranean based on 7-year observations, J. Geophys. Res.-Atmos., 110, D15309, doi:10.1029/2005JD005991, 2005.

Gordon, H., Kirkby, J., Baltensperger, U., Bianchi, F., Breitenlechner, M., Curtius, J., Dias, A., Dommen, J., Donahue, N. M., Dunne, E. M., Duplissy, J., Ehrhart, S., Flagan, R. C., Frege, C., Fuchs, C., Hansel, A., Hoyle, C. R., Kulmala, M., Kürten, A.,Lehtipalo, K., Makhmutov, V., Molteni, U., Rissanen, M. P., Stozkhov, Y., Tröstl, J., Tsagkogeorgas, G., Wagner, R., Williamson, C., Wimmer, D., Winkler, P. M., Yan, C., and Carslaw, K. S.: Causes and importance of new particle formation in the present-day and preindustrial atmospheres, J. Geophys. Res. Atmos., 122, 8739–8760, doi:10.1002/2017JD026844, 2017.

Ghan, S. J., Abdul-Razzak, H., Nenes, A., Ming, Y., Liu, X., Ovchinnikov, M., Shipway, B., Meskhidze, N., Xu, J., and Shi, X.: Droplet Nucleation: Physically-based Parameterization and Comparative Evaluation, J. Adv. Model. Earth Syst., 3, M10001, doi:10.1029/2011MS000074, 2011.

Hermann, M., Heintzenberg, J., Wiedensohler, A., Zahn, A., Heinrich, G., and Brenninkmeijer C. A. M.: Meridional distribution of aerosol particle number concentrations in the upper troposphere and lower stratosphere obtained by Civil Aircraft for Regular Investigation ofthe Atmosphere Based on an Instrument Container (CARIBIC) flights,J. Geophys. Res.,108(D3), 4114, doi:10.1029/2001JD001077, 2003.

Hudson, J. G., and Noble, S.: CCN and vertical velocity influences on droplet concentrations and supersaturations in clean and polluted stratus clouds, Journal of the Atmos. Sciences, Volume 71, doi.org/10.1175/JAS-D-13-086.1, 2014.

Hussein, T., Puustinen, A., Aalto, P. P., Mäkelä, J. M., Hämeri, K., and Kulmala, M.: Urban aerosol number size distributions, Atmos. Chem. Phys., 4, 391-411, https://doi.org/10.5194/acp-4-391-2004, 2004.

Hussein, T., Dal Maso, M., Petäjä, T., Koponen, I., Paatero, P., Aalto, P., Hämeri, K., Kulmala, M.: Evaluation of an automatic algorithm for fitting the particle number size distributions. Boreal Env.Res., 10, 337-355, 2005.

Kalivitis, N., Kerminen, V.-M., Kouvarakis, G., Stavroulas, I., Bougiatioti, A., Nenes, A., Manninen, H. E., Petäjä, T., Kulmala, M., and Mihalopoulos, N.: Atmos. Chem. Phys., 15, 9203-9215, doi:10.5194/acp-15-9203-2015, 2015.

Kalivitis, N., Kerminen, V.-M., Kouvarakis, G., Stavroulas, I., Tzitzikalaki, E., Kalkavouras, P., Daskalakis, N., Myriokefalitakis, S., Bougiatioti, A., Manninen, H. E., Roldin, P., Petäjä, T., Boy, M., Kulmala, M., Kanakidou, M., and Mihalopoulos, N.: Formation and growth of atmospheric nanoparticles in the eastern Mediterranean: results from long-term measurements and process simulations, Atmos. Chem. Phys. Discuss., doi:10.5194/acp-2018-229, 2018.

Kalkavouras, P., Bossioli, E., Bezantakos, S., Bougiatioti, A., Kalivitis, N., Stavroulas, I., Kouvarakis, G., Protonotariou, A. P., Dandou, A., Biskos, G., Mihalopoulos, N., Nenes, A., and Tombrou, M.: New particle formation in the southern Aegean Sea during the Etesians: importance for CCN production and cloud droplet number, Atmos. Chem. Phys.,17, 175-192, doi:10.5194/acp-17-175-2017.

Katoshevski, D., Nenes, A., Seinfeld, J. H.: A Study of processes that govern the maintenance of aerosols in the marine boundary layer, Volume 30, Issue 4, 503-532, doi:10.1016/S0021-8502(98)00740-X, 1999.

Kerminen, V.-M., Paramonov, M., Antilla, T., Riipinen, I., Fountoukis, C., Korhonen, H., Asmi, E., Laakso, L., Lihavainen, H., Swietlicki, E., Svenningsson, B., Asmi, A., Pandis, S.N., Kulmala, M., and Petäjä, T.: Cloud condensation nuclei production associated with atmosphericnucleation: a synthesis based on existing literature and new results, Atmos. Chem. Phys., 12, 12037–12059, doi:10.5194/acp-12-12037-2012, 2012.

Kreidenweis, S. M., Penner, J. E., Yin, F., and Seinfeld, J. H.: The effects of dimethylsulfide upon marine aerosol concentrations, Atm. Environ., Vol. 25A, No.11, pp. 2501-2511, 1991.

Kulmala, M. and Kerminen, V.-M.: On the formation and growth ofatmospheric nanoparticles, Atmos. Res., 90, 132–150, 2008.

Kulmala, M., Petäjä, T., Nieminen, T., Sipilä, M., Manninen, H. E., Lehtipalo, K., Dal Maso,M., Aalto, P., Junninen, H., Paasonen, P., Riipinen, I., Lehtinen, K. E. J., Laaksonen, A., and Kerminen, V.-M.: Measurement of the nucleation of atmospheric aerosol particles, Nat. Protocol., 7, 1651–1667, doi:10.1038/nprot.2012.091, 2012.

Ma, N., Zhao, C., Tao, J., Wu, Z., Kecorius, S., Wang, Z., Größ, J., Liu, H., Bian, Y., Kuang, Y., Teich, M., Spindler, G., Müller, K., Pinxteren, D., Herrmann, H., Hu, M., and Wiedensohler, A.: Variation of CCN activity during new particle formation events inthe North China Plain, Atmos. Chem. Phys., 16, 8593–8607, doi:10.5194/acp-16-8593-2016, 2016.

Merikanto, J., Spracklen, D. V., Mann, G. W., Pickering, S. J., and Carslaw, K. S.:Impact of nucleation on global CCN, Atmos. Chem. Phys., 9, 8601–8616, doi:10.5194/acp-9-8601-2009 2009.

Meskhidze, N., Nenes, A., Conant, W. C., and Seinfeld, J. H.: Evaluation of a new Cloud Droplet Activation Parameterization withIn Situ Data from CRYSTAL-FACE and CSTRIPE, J. Geophys.Res., 110, D16202, doi:10.1029/2004JD005703, 2005.

Mihalopoulos, N., Stephanou, E., Kanakidou, M., Pilitsidis, S., and Bousquet, P.: Tropospheric aerosol ionic composition in the Eastern Mediterranean region, Tellus B, 49, 314–326, 1997.

Morales, R. and Nenes, A.: Characteristic updrafts for computing distribution-averaged cloud droplet number and stratocumulus cloud properties, J. Geophys. Res., 115, D18220, doi:10.1029/2009JD013233, 2010.

Morales, R., Nenes, A., Jonsson, H., Flagan, R. C. and Seinfeld, J. H.: Evaluation of a diabatic droplet activation parameterization using in-situ cloud data, J. Geoph. Res., 116, D15205, doi:10.1029/2010JD015324, 2011.

730 Morales Betancourt, R. and Nenes, A.: Droplet activation parameterization: the population-splitting concept revisited, Geosci. Model Dev., 7, 2345–2357, doi:10.5194/gmd-7-2345-2014, 2014.

Nenes, A. and Seinfeld, J. H.: Parameterization of cloud droplet formation in global climate models, J. Geophys. Res, 108, 4415, doi:10.1029/2002JD002911, 2003.

735

Ng, N. L., Herndon, S. C., Trimborn, A., Canagaratna, M. R.,Croteau, P. L., Onasch, T. B., Sueper, D., Worsnop, D. R., Zhang, Q., Sun, Y. L., and Jayne, J. T.: An Aerosol Chemical Speciation Monitor (ACSM) for routine monitoring of the composition and mass concentrations of ambient aerosol, Aerosol Sci. Technol.,45, 770–784, doi:10.1080/02786826.2011.560211,

740 2011.

Lance, S., Nenes, A., Medina, J., and Smith, J. N.: Mapping the operation of the DMT continuous flow CCN counter, Aerosol Science and Technology, 40:4, 242-254, DOI: 10.1080/02786820500543290, 2006.

Lathem, T. L., and Nenes, A.: Water vapor depletion in the DMT continuous-flow CCN

745 chamber: effects on supersaturation and droplet growth, Aerosol Science and Technology, 45:5, 604-615, DOI: 10.1080/02786826.2010.551146, 2011.

Leino, K., Nieminen, T., Manninen, H. E., Petäjä, T., Kerminen, V.-M., and Kulmala, M.: Intermediate ions as a strong indicator of new particle formation bursts in a boreal forest, Boreal Environ. Res., 21, 274–286, 2016.

750 O'Dowd, C. D., Hämeri, K., Mäkelä, J. M., Pirjola, L., Kulmala, M., Jennings, S. G., Berresheim, H., Hansson, H.-C., Leeuw, G., Kunz, G. J., Allen, A. G., Hewitt, C. N., Jackson, A., Viisanen, Y., and Hoffmann, T.: A dedicated study of new Particle Formation and Fate in the Coastal Environment (PARFORCE): Overview of objectives and achievements, J. Geophys. Res., 107, D19, 8108, doi:10.1029/2001JD000555, 2002.

755 Paasonen, P., Peltola, M., Kontkanen, J., Junninen, H., Kerminen, V.-M., and Kulmala, M.: Comprehensive analysis of particle growth rates from nucleation mode to cloud condensation nuclei in boreal forest, Atmos. Chem. Phys., 18, 12085–12103, doi:10.5194/acp-18-12085-2018, 2018.

Peng, J. F., Hu, M., Wang, Z. B., Huang, X. F., Kumar, P., Wu, Z. J., Guo, S., Yue, D. L.,

760 Shang, D. J., Zheng, Z., and He L. Y.: Submicron aerosols at thirteen diversified sites in China: size distribution, new particle formation and corresponding contribution to cloud condensation nuclei production, Atmos. Chem. Phys., 14, 10249–10265, doi:10.5194/acp-14-10249-2014 2014.

Petters, M. D. and Kreidenweis, S. M.: A single parameter representation of hygroscopic growth and cloud condensation nucleusactivity, Atmos. Chem. Phys., 7, 1961–1971, doi:10.5194/acp-7-1961-2007, 2007.

Pierce, J. R. and Adams, P. J.: Efficiency of cloud condensation nuclei formation from ultra-fine particles, Atmos. Chem. Phys., 7, 1367–1379, doi:10.5194/acp-7-1367-2007, 2007.

Pöschl, U., Martin, S. T., Sinha, B., Chen, Q., Gunthe, S. S., Huffman, J. A., Borrmann, S., Farmer, D. K., Garland, R. M., Helas, G., Jinemez, J. L., King, S. M., Manzi, A., Mikhailov, E., Pauliquevis, T., Petters, M. D., Prenni, A. J., Roldin, P., Rose, D., Schneider, J., Su, H., Zorn, S. R., Artaxo, P., and Andreae, M. O.: Rainforest aerosols as biogenic nuclei of clouds and precipitation in the Amazon, Science, Vol. 329, Issue 5998, pp. 1513-1516, DOI: 10.1126/science.1191056, 2010.

Roberts, G. C. and Nenes, A.: A Continuous-Flow Streamwise Thermal-Gradient CCN Chamber for Atmospheric Measurements, Aerosol Sci. Technol., 39, 206–221, 2005.

Rose, C., Sellegri, K., Moreno, I., Velarde, F., Ramonet, M., Weinhold, K., Krejci, R., Andrade, M., Wiedensohler, A., Ginot, P., and Laj, P.: CCN production by new particle formation in the free troposphere, Atmos. Chem. Phys., 17, 1529–1541, doi:10.5194/acp-17-1529-2017, 2017.

Rosenfeld, D., Kaufman, Y. J, and Koren, I.: Switching cloud cover and dynamical regimes from open to closed Benard cells in response to the suppression of precipitation by aerosols, Atmos. Chem. Phys., 6, 2503-2511, doi:10.5194/acp-6-2503-2006, 2006.

Seinfeld, J. and Pandis, S. (Eds.): Atmospheric Chemistry and Physics: From Air Pollution to Climate Change, 2nd Edn., JohnWiley, edited by: Hoboken, N. J., ISBN: 978-0-471-72018-8,1232 pp., 2006.

Seinfeld, J. H., Bretherton, C. S., Carslaw, K. S., Coe, H., DeMott, P. J., Dunlea, E. J., Feingold, G., Ghan, S. J., Guenther, A. B., Kahn, R. A., Kracunas, I. P., Kreidenweis, S. M., Molina, M. J., Nenes, A., Penner, J. E., Prather, K. A., Ramanathan, V., Ramaswamy, V., Rasch, P. J., Ravishankara, A. R., Rosenfeld, D., Stephens, G., Wood R.: Improving Our Fundamental Understanding of the Role of Aerosol-Cloud Interactions in the Climate System, Proc.Nat.Acad.Sci, 113, 21, 5781-5790, doi: 10.1073/pnas.151404311, 2016.

Sihto, S.-L., Mikkilä, J., Vanhanen, J., Ehn, M., Liao, L., Lehtipalo, K., Aalto, P. P., Duplissy, J., Petäjä, T., Kerminen, V.-M., Boy, M., and Kulmala, M.: Seasonal variation of CCN concentrations and aerosol activation properties in boreal forest, Atmos. Chem. Phys., 11, 13269–13285, doi:10.5194/acp-11-13269-2011, 2011.

Spracklen, D. V., Carslaw, K. S., Kulmala, M., Kerminen, V.-M., Sihto, S.-L., Riipinen, I., Merikanto, J., Mann, G. W., Chipperfield, M. P., Wiedensohler, A., Birmili, W., and

Lihavainen, H.: Contribution of particle formation to global cloud condensation nuclei concentrations, Geophys. Res. Lett., 35, L06808, doi:10.1029/2007GL033038, 2008a.

Spracklen, D. V., Bonn, B., and Carslaw, K. S.: Boreal forests, aerosols and the impacts of clouds and climate, Phil. Trans.Royal Soc. A., 366, 4613–4626, 2008b.

Stein A, F., Draxler, R. R, Rolph, G. D., Stunder, B. J. B., Cohen, M.D., and Ngan, F.: NOAA's HYSPLIT atmospheric transport and dispersion modeling system, B.Am.Meteorol.Soc.,96, 2059–2077, doi:10.1175/BAMS-D-14-00110.1, 2015.

Stevens, B. and Feingold, G.: Untangling aerosols effects on cloudsand precipitation in a buffered system, Nature, 461, 607–613, doi:10.1038/nature08281, 2009.

Sullivan, S.C., Lee, D., Oreopoulos, L., and Nenes, A.: The role of updraft velocity in temporal variability of cloud hydrometeor number, Proc.Nat.Acad. Sci., 113, 21, 5781-5790, doi:10.1073/pnas.1514043113, 2016.

Sullivan, R. C., Crippa, P., Matsui, H., Leung, L. R, Zhao, C., Thota, A., and Pryor, S. C.: New particle formation leads to cloud dimming, Climate and Atmospheric Science (2018) 1:9; doi:10.1038/s41612-018-0019-7, 2018.

Tombrou, M., Bossioli, E., Kalogiros, J., Allan, J. D., Bacak, A., Biskos, G., Coe, H., Dandou, A., Kouvarakis, G., Mihalopoulos, N., Percival, C. J., Protonotariou, A. P., and Szabó-Takács, B.: Physical and chemical processes of airmasses in the Aegean Sea during Etesians: Aegean-GAME airborne campaign, Sci. Total Environ., 506–507, 201–216, doi:10.1016/j.scitotenv.2014.10.098, 2015.

Tunved, P., Hansson, H.-C., Kerminen, V.-M., Ström, J., Dal Maso, M., Lihavainen, H., Viisanen, Y., Aalto, P. P., Komppula, M., and Kulmala, M.: High Natural Aerosol Loading Over Boreal Forests, Science, 312, 261–263, doi:10.1126/science.1123052, 2006.

Vaattovaara, P., Huttunen, P. E., Yoon, Y. J., Joutsensaari, J., Lehtinen, K. E. J., O'Dowd, C. D., and Laaksonen, A.: The composition of nucleation and Aitken modes particles during coastal nucleation events: evidence for marine secondary organic contribution, Atmos. Chem. Phys., 6, 4601–4616, doi:10.5194/acp-6-4601-2006, 2006.

Wang, Q., Zhao, J., Du, W., Ana, G., Wang, Z., Sun, L., Wang, Y., Zhang, F., Li, Z., Ye, X., Sun, Y.: Characterization of submicron aerosols at a suburban site in central China. Atmos. Environ. 131, 115–12, doi:10.1016/j.atmosenv.2016.01.054, 2016.

Westervelt, D. M., Pierce, J. R., Riipinen, I., Trivitayanurak, W., Hamed, A., Kulmala, M., Laaksonen, A., Decesari, S., and Adams, P. J.: Formation and growth of nucleated particles into

cloud condensation nuclei: model–measurement comparison, Atmos. Chem. Phys., 13, 7645–7663, doi:10.5194/acp-13-7645-2013, 2013.

Westervelt, D. M., Pierce, J. R., and Adams, P. J.: Analysis of feedbacks between nucleation rate, survival probability and cloud condensation nuclei formation, Atmos. Chem. Phys., 14, 5577–5597, doi:10.5194/acp-14-5577-2014, 2014.

Wiedensohler, A, Chen, Y. F., Nowak, A, Wehner, B., Achtert, P., Berghof, M., Birmili, W., Wu, Z. J., Hu, M., Zhu, T., Takegawa, N., Kita, K., Kondo, Y., Lou, S. R., Hofzumahaus, A., Holland, F., Wahner, A., Gunthe, S. S, Rose, D., Su, H., and Pöschl, U.: Rapid aerosol particle growth and increase ofcloud condensation nucleus activity by secondary aerosol formation and condensation: A case study for regional air pollutionin northeastern China, J. Geophys. Res., 114, D00G08, doi:10.1029/2008JD010884, 2009.

Wiedensohler, A., Birmili, W., Nowak, A., Sonntag, A., Weinhold, K., Merkel, M., Wehner, B., Tuch, T., Pfeifer, S., Fiebig, M., Fjäraa, A. M., Asmi, E., Sellegri, K., Depuy, R., Venzac, H., Villani, P., Laj, P., Aalto, P., Ogren, J. A., Swietlicki, E., Williams, P., Roldin, P., Quincey, P., Hüglin, C., Fierz-Schmidhauser, R., Gysel, M., Weingartner, E., Riccobono, F., Santos, S., Grüning, C., Faloon, K., Beddows, D., Harrison, R., Monahan, C., Jennings, S. G., O'Dowd, C. D., Marinoni, A., Horn, H.-G., Keck, L., Jiang, J., Scheckman, J., McMurry, P. H., Deng, Z., Zhao, C.S., Moerman, M., Henzing, B., de Leeuw, G., Löschau, G., and Bastian, S.: Mobility particle size spectrometers: harmonization of technical standards and data structure to facilitate high quality long-term observations of atmospheric particle number size distributions, Atmos. Meas. Tech., 5, 657–685, doi:10.5194/amt-5-657-2012, 2012.

Wu, Z.J., Poulain, L., Birmili, W., Größ, J., Niedermeier, N., Wang, Z. B., Herrmann, H., and Wiedensohler, A.: Some insights into the condensing vapors driving new particle growth to CCN sizes on the basis of hygroscopicity measurements, Atmos. Chem. Phys., 15, 13071–13083, doi:10.5194/acp-15-13071-2015, 2015.

Zhang, Q., Stanier, C. O., Canagaratna, M. R., Jayne, J. T., Worsnop, D. R., Pandis, S. N., and Jimenez, J. L.: Insights intothe Chemistry of New Particle Formation and Growth Events in Pittsburgh Based on Aerosol Mass Spectrometry, Environ. Sci.Technol., 38, 4797–4809, doi:10.1021/es035417u, 2004.

Atmos. Chem. Phys. Discuss., https://doi.org/10.5194/acp-2018-1254
Manuscript under review for journal Atmos. Chem. Phys.
Discussion started: 11 December 2018

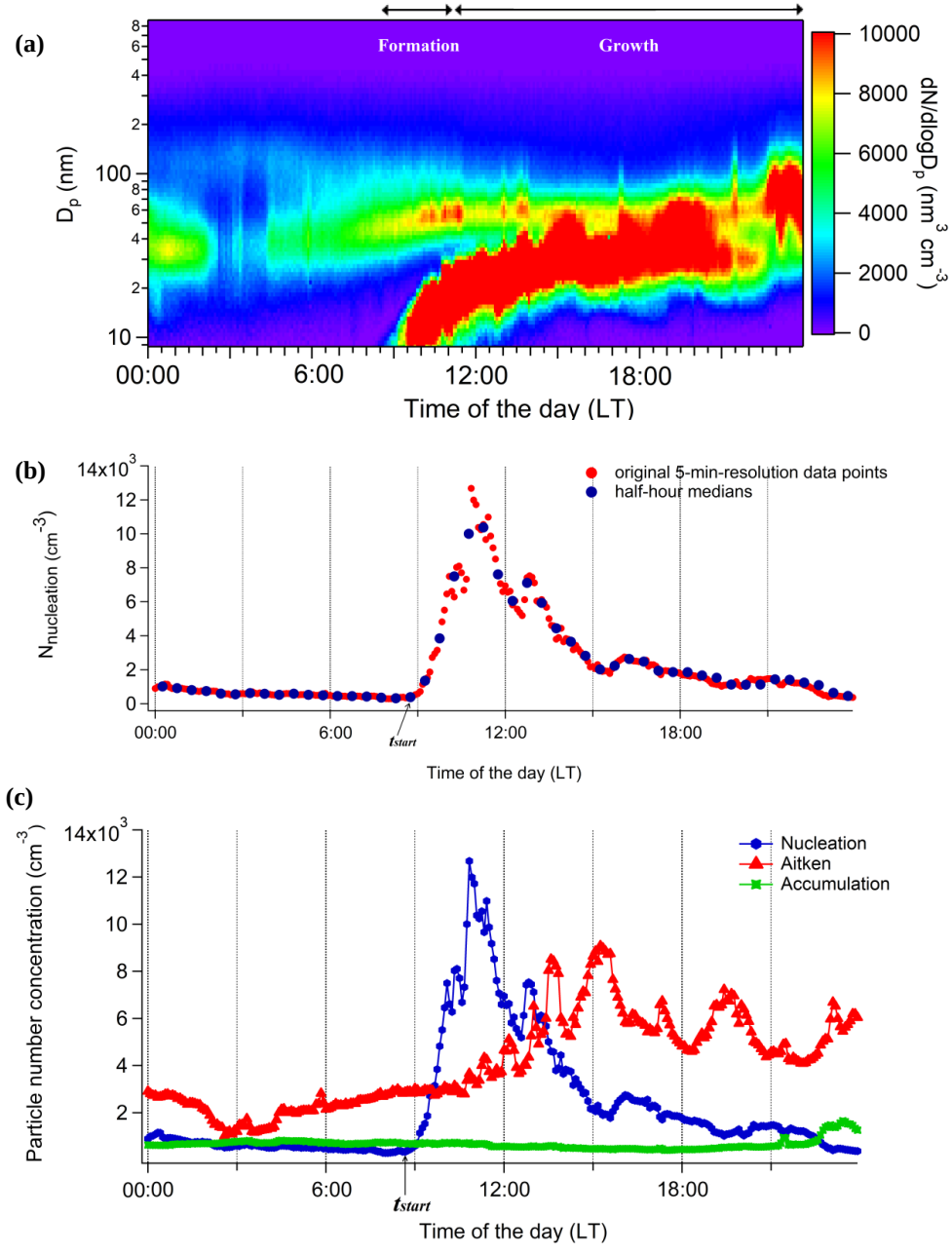

Figure 1. A "representative" new particle formation event captured at Finokalia on 29 August 2012. **(a)** Diurnal evolution of the aerosol size distribution, **(b)** differences between 5-min-resolution original points (red dots) and calculated half-hour median concentrations of particles in size range of 9-25 nm (blue dots), and **(c)** diurnal evolution of nucleation (blue line), Aitken (red line), and accumulation mode particle number concentration (green line), respectively.

Atmos. Chem. Phys. Discuss., https://doi.org/10.5194/acp-2018-1254
Manuscript under review for journal Atmos. Chem. Phys.
Discussion started: 11 December 2018

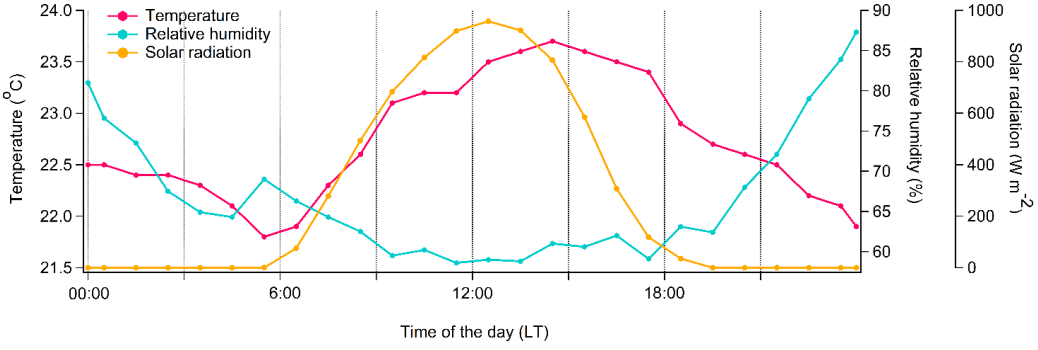

Figure 2. Diurnal evolution of the temperature (purple line), relative humidity (light blue), and solar radiation (orange line), respectively during the "representative" new particle formation event observed at Finokalia on 29 August 2012.

Atmos. Chem. Phys. Discuss., https://doi.org/10.5194/acp-2018-1254
Manuscript under review for journal Atmos. Chem. Phys.
Discussion started: 11 December 2018

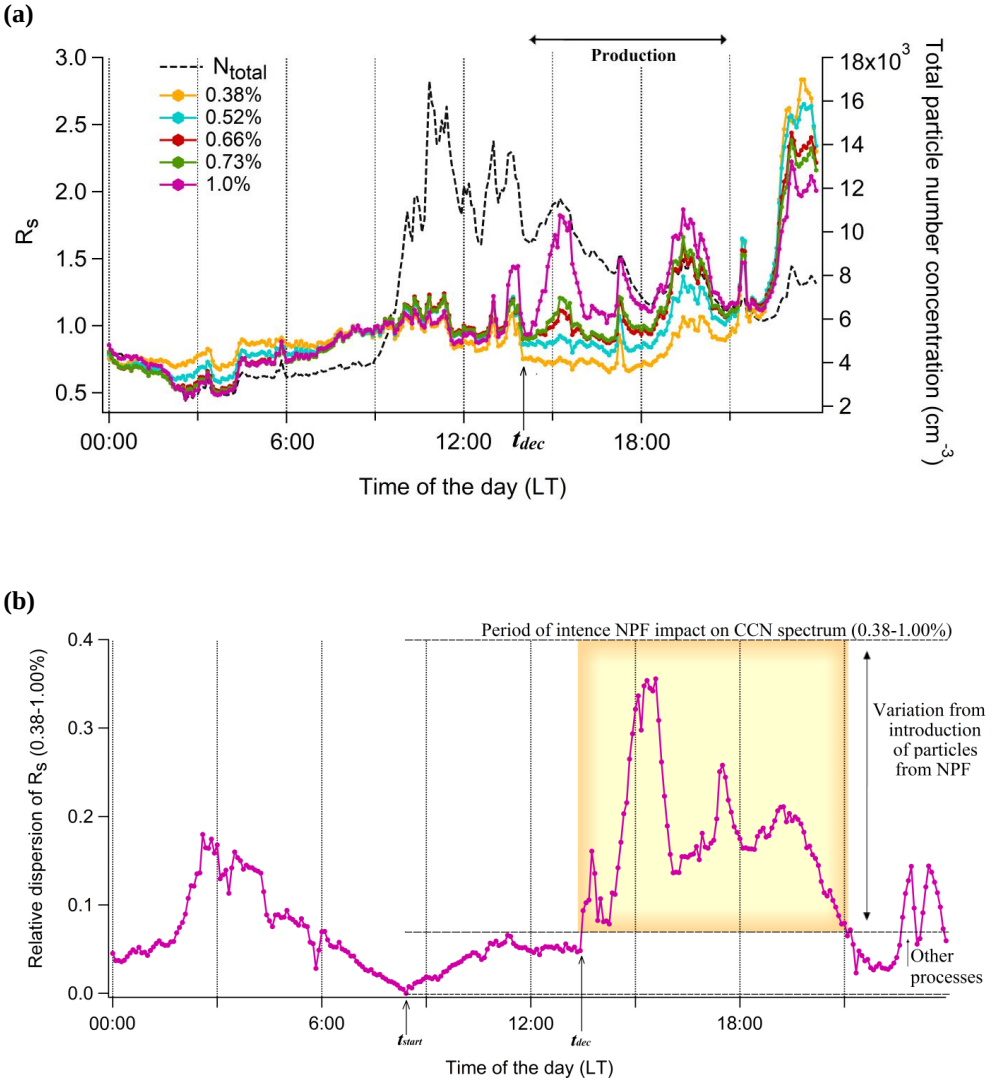

Figure 3. (a) Diurnal evolution of the R_s for supersaturation 0.38 (orange line), 0.52 (light blue line), 0.66 (red line), 0.73 (green line), and 1.0 % (purple line) (left axis) respectively, and total particle number concentrations, N_{total} (black line-right axis) during the "representative" new particle formation event captured at Finokalia on 29 August 2012. **(b)** Diurnal evolution of the relative dispersion of the R_s for all supersaturations (s) (0.38 to 1.0 %) during the "representative" new particle formation event captured at Finokalia on 29 August 2012. t_{start} (08:30 LT) is the starting time of the NPF event, while t_{dec} is the "decoupling time" (13:30 LT), when the NPF episode start to influence the CCN concentrations according to the approach described in the main text. The period of intense NPF event on CCN spectrum for all s is shaded in yellow.

Atmos. Chem. Phys. Discuss., https://doi.org/10.5194/acp-2018-1254
Manuscript under review for journal Atmos. Chem. Phys.
Discussion started: 11 December 2018

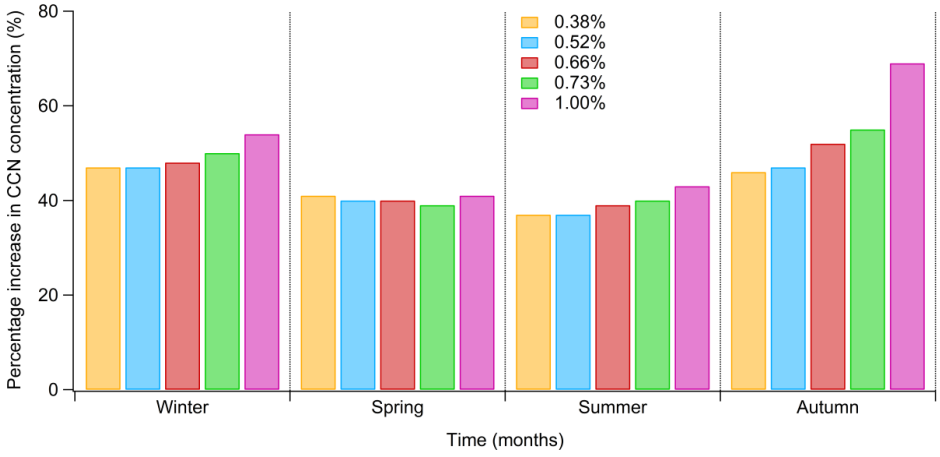

Figure 4. Seasonal variation of percentage increase regarding the estimated CCN concentrations for supersaturation 0.38 (orange bars), 0.52 (light blue bars), 0.66 (red bars), 0.73 (green bars), and 1.0 % (purple bars), respectively, relative to the available 162 NPF days at Finokalia, throughout the period June 2008-May 2015.

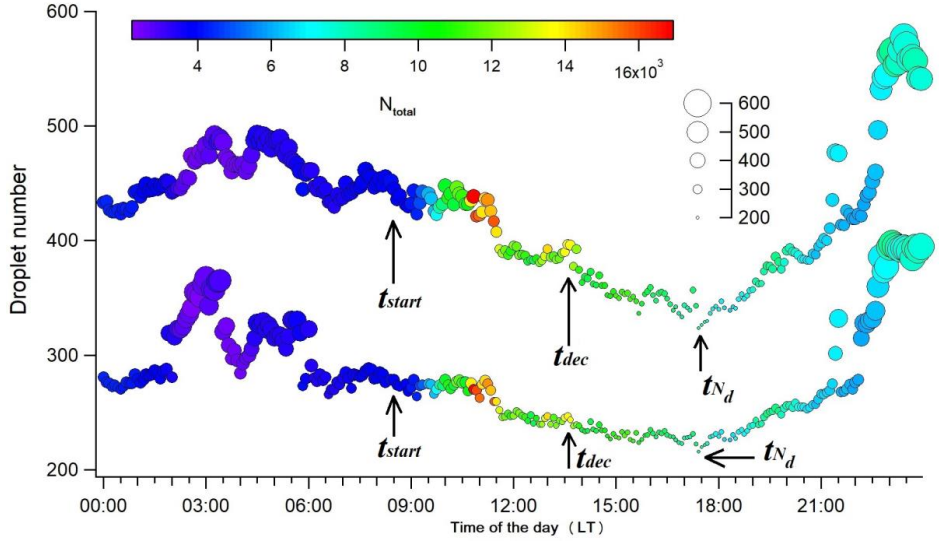

Figure 5. Diurnal evolution of the total aerosol particle number concentrations in cm^{-3} (N_{total}– color bar) and calculated cloud droplet number concentrations (N_d) (left axis) for updraft velocities of σ_w= 0.3 m s^{-1} (bottom), and σ_w=0.6 m s^{-1} (top) during the "representative" new particle formation event captured at Finokalia on 29 August 2012. The size of the circles corresponds to the number concentration of N_d, while t_{dec} is the "decoupling time" (13:30 LT), and t_{Nd} is the time when the number of droplets start to "feel" the NPF (17:25 LT), according to the approach described in the main text.

Atmos. Chem. Phys. Discuss., https://doi.org/10.5194/acp-2018-1254
Manuscript under review for journal Atmos. Chem. Phys.
Discussion started: 11 December 2018

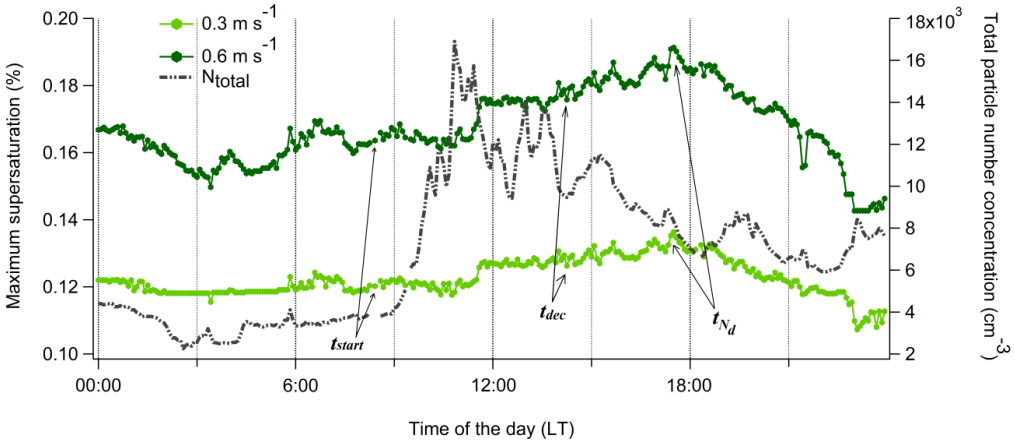

Figure 6. Diurnal evolution of the calculated maximum supersaturation (s_{max}) (lest axis) and total aerosol particle number concentrations (N_{total}) (right axis) for updraft velocities of σ_w= 0.3 m s^{-1}, and σ_w=0.6 m s^{-1} during the "representative" new particle formation event captured at Finokalia on 29 August 2012.